https://doi.org/10.5194/wes-2024-146
Preprint. Discussion started: 2 December 2024

eawe european academy of wind energy
Open Access WIND ENERGY SCIENCE DISCUSSIONS

Improved coupling between an atmospheric LES and an aeroelastic code for the simulation of wind turbines under heterogeneous inflow

Sonja Steinbrück[1,2], Thorben Eilers[1], Lukas Vollmer[2], Kerstin Avila[1], and Gerald Steinfeld[1]

[1]ForWind, Institute of Physics, Carl von Ossietzky University Oldenburg, Küpkersweg 70, 26129 Oldenburg, Germany
[2]Fraunhofer Institute for Wind Energy Systems IWES, Küpkersweg 70, 26129 Oldenburg, Germany

Correspondence: Sonja Steinbrück (sonja.steinbrueck@iwes.fraunhofer.de)

Abstract. Wind energy simulations face a central challenge of coupling length scales, ranging from wind fields spanning hundreds of kilometers to the centimeter-scale relevant for turbine dynamics. To address this challenge, simulations employ fundamentally different tools. For instance, a large-eddy simulation tool simulates the large scales, while an aeroelastic code captures wind-turbine interaction at smaller scales. This study aims to examine a model framework developed to investigate wind turbine behavior in heterogeneous wind fields, such as those found in wind farms. The framework combines FAST and PALM, simulating realistic atmospheric wind conditions while providing high-quality turbine information. Computational efficiency is ensured through the use of a decoupled time step, resulting in an Actuator Sector Model within PALM and a blade-element momentum approach in FAST. Additionally, a wind speed correction is implemented to reduce errors that are caused by the necessary smearing of forces on the numerical grid of the atmospheric simulation when using actuator models to account for wind turbine effects. Results are evaluated through comparisons of different model setups and turbine measurements, including an assessment of a wake situation involving two turbines. Special attention is given to the number of blade elements in the turbine setup. The proposed model framework demonstrates good agreement with measurement data and performs well in the wake situation, used as representative of a highly heterogeneous wind field. It is applicable for studying turbine loads and power output in wake situations and other atmospheric wind fields.

1 Introduction

In wind energy, precise predictions of power output, loads, and wake effects of wind turbines are crucial for optimizing safety margins in their construction and site selection, ultimately leading to reduced energy costs. An acurate prediction requires information describing wind fields on a scale of several kilometers down to centimeters, along with turbine movements at the centimeter scale. Numerical simulations are an essential tool in wind energy research. They enable the study of a wide range of applications and scenarios under controlled conditions. Typical applications are simulations of entire wind farms or the investigation of loads acting on single wind turbines (Churchfield et al., 2012; Storey et al., 2016; Mehta et al., 2014). One major challenge is the representation of the wind turbine in the flow field, as this can be computationally very expensive if e.g. the flow at the rotor blades is resolved. On the other hand, a high quality of information on the turbine is usually desired.

https://doi.org/10.5194/wes-2024-146
Preprint. Discussion started: 2 December 2024

eawe european academy of wind energy
Open Access WIND ENERGY SCIENCE DISCUSSIONS

State-of-the-art turbine model concepts.

Different approaches have been developed to represent the effect of a wind turbine in computational fluid dynamics (CFD) models, each with varying quality of results and computational demand. For instance, the Actuator Disk Model (ADM(R)), which can be used with or without rotation, and the Actuator Line Model (ALM), which represents rotor blades as lines. Models, such as the Actuator Sector Model (ASM) which represents the turbine as circle segments, bridge the gap between ALM and ADM(R) (Storey et al., 2015; Krüger et al., 2022). The computational costs for an ADM without rotation are comparatively low, providing good quality results in the far wake for mean wind speeds. However, it cannot provide the double Gaussian structure of the wind field in the near wake and cannot resolve quantities along the blade. The ALM on the other hand provides more detailed turbine information, such as loads along the blades and tower, but requires significantly more computational resources due to the limitation of the time step by the rotor speed. The ASM representation can be a compromise between these models, providing detailed turbine output while significantly enhancing computational efficiency compared to the ALM (Krüger et al., 2022).

Model Framework as presented in Krüger et al. (2022).

In Krüger et al. (2022) a newly developed model framework is described between the aeroelastic code FAST (fatigue, aerodynamics, structures, and turbulence, Jonkman and Buhl Jr. (2005)) and the large-eddy simulation (LES) tool PALM (parallelised large-eddy simulation model, Maronga et al. (2020)), where a sector shaped representation is used on the side of the LES model, while FAST retains its blade element momentum (BEM) representation. This combination enables efficient calculations with a high resolution and quality of the turbine output. Additionally, the computational speed of the ASM coupled with an LES model is far higher than that of an ALM in a similar coupling. In Krüger et al. (2022) the reduction of computational time for an exemplary case is 89%. To address inaccuracies in calculating turbine forces using wind speeds within the rotor area the coupling method utilizes the free inflow wind speeds outside of the rotor's induction zone. It incorporates the SWIRL induction model of FAST to determine the wind speeds at positions along the rotor line. The induction model assumes the validity of Taylor's frozen eddy hypothesis (Taylor, 1938; Moriarty and Hansen, 2005) when calculating the wind speeds that reach the turbine.

The coupling between PALM and FAST Krüger et al. (2022), from now on denoted as ASM SWIRL, was validated with simulation data of the generic NREL 5 MW turbine (Jonkman et al., 2009b) and to measurements of an eno114 3.5 MW turbine. A good agreement between modelled and measured load spectra and power output was observed. In addition, the method was tested in a benchmark case against other models of different fidelity (Doubrawa et al., 2020) confirming its reliability in a free inflow situation.

Limits of ASM SWIRL and other models.

The assumption of the SWIRL induction model does not hold in situations where the flow is temporally and spatially heterogeneous upstream of the turbine, such as a turbine in the wake of another turbine. Additionally, the method ASM SWIRL incorporates a time offset, utilizing wind speeds in front of the wind turbine to determine power at the rotor plane. For varying

https://doi.org/10.5194/wes-2024-146
Preprint. Discussion started: 2 December 2024

eawe european academy of wind energy
Open Access WIND ENERGY SCIENCE DISCUSSIONS

inflow conditions and to avoid the time offset it is necessary to use the wind speeds within the rotor area, which requires correction due to potential errors. Wind speeds must be interpolated to the blade positions, which can result in imprecise values depending on grid size. This arises from simplifying the blade to lines, deviating from the intended lifting line theory (Dag, 2017).

Furthermore, to assure numerical stability and to have the forces from the turbine at the grid positions, where u, v and w are defined, the turbine models, i.e. ALM, ADM(R) and ASM, generally use a Gaussian shaped projection of the aerodynamic forces (Sørensen et al., 1998). The force distribution can be influenced by a smearing coefficient, whose lower limit is bound to the grid size (Troldborg, 2008). However, it also influences the velocities at the blades (Mikkelsen, 2003) and therefore also the turbine model behaviour. This makes this parameter an important adjustment factor.

In Martínez-Tossas et al. (2017), an analytical approach is described to optimize the smearing coefficient to ensure numerical stability and reliable results of the turbine response. The smearing coefficient was determined by comparing the velocity field to a desired potential velocity field of a uniform inflow. It was concluded that the smearing coefficient depends on the ratio of the grid size to the blade's chord length. This poses the problem for each simulation, using different turbine models and model domains, that the smearing coefficient has to be determined.

In Mohammadi et al. (2024) an empirical approach is presented. Similar to Krüger et al. (2022), an LES code is coupled with an ASM. However, the universal application of the presented framework has not yet been tested.

Explanation of the implemented correction.

An alternative approach, with the potential for universal application in addressing inaccuracies in blade velocities due to force projection, is described in Dag (2017) and followed up in Meyer Forsting et al. (2019). These authors identified the root cause of the problem. The ALM representation developed by (Sørensen and Shen, 2002) of a turbine is intended as a lifting line method. However, due to the numerical requirements, the Gaussian shaped distribution of the forces is chosen, which does not represent the lifting line theory entirely (Dag, 2017). To counteract, Dag (2017) proposes a correction based on the dynamic near-wake model, described in Pirrung et al. (2016, 2017a, b), with a viscous core model (Lamb, 1932; Oseen, 1911).

In Meyer Forsting et al. (2019) the deficits of the Gaussian smearing used in ALM are discussed and a solution based on the considerations described in (Dag, 2017) is presented. According to Dag (2017) the discrepancy between the lifting line theory and the Gaussian shaped smearing can be reduced by considering the Lamb-Oseen vortex. Meyer Forsting et al. (2019) demonstrated that the correction mentioned above leads to improved results for the NREL 5 MW turbine, with the throwback to be computationally costly. To address this, Meyer Forsting et al. (2020) proposed a reduced version of the correction that significantly decreases computational time, while maintaining the quality of the corrected results. As a result, this method proves to be a valuable addition to existing ALM codes, as it does not significantly increase overall calculation time. The correction method proposed in Meyer Forsting et al. (2020) is from now on denoted as NWC (near-wake correction).

Objective.

The aim of this work is to create an efficient modelling framework that combines simulations of atmospheric flows with de-

https://doi.org/10.5194/wes-2024-146
Preprint. Discussion started: 2 December 2024

tailed turbine performance, ensuring applicability to a variety of wind conditions and independence from the model setup. To reach this goal, we transfer the NWC from an ALM application to an ASM method, building upon the model framework established by Krüger et al. (2022), as the computational efficiency of the ASM coupled with an LES model is far higher than an ALM in a similar coupling. The application scope of the FAST-PALM model system is enhanced, enabling simulations of turbines in horizontally heterogeneous flow conditions, with the same high level of detail as an ALM with NWC but at a reasonable computational speed. The method is investigated in laminar and turbulent flow and validated against measurement data.

Structure of the paper.

Section 2 outlines the modifications and adaptations necessary for applying the ALM-based NWC to the ASM. In Section 3, the implemented methods are evaluated under laminar, turbulent flow, and wake conditions. Section 4 presents a comparison of the model framework with measurement data. In the Appendix section A, the impact of blade resolution on the results is examined in greater detail.

2 Methodology: Extension of the PALM-FAST coupling to include NWC

In simulations using an ALM, the Gaussian force smearing incorporates the Lamb-Oseen viscous core, which is present in both bound and trailed vorticity. The presence of the viscous core in the vortex leads to lower induced velocities near the vortex center when compared to the inviscid solution of the lifting line theory, which serves as the theoretical foundation for the ALM. As a result, the trailed vorticity induced by an ALM results in larger angle of attacks and increased forces at the blades. To address and recover this missing induction, the NWC method combines a near-wake model of the trailed vorticity with the Lamb-Oseen viscous core model. This is achieved by utilizing the correlation between the smearing length scale ε and the radius of the viscous core. For each trailed vortex between blade elements, its distance to all elements on the blade is determined in each time step, and the correction value is calculated based on its circulation strength and viscous core size. The induced velocities of such vortices change at each time step due to blade rotation, flow convection, and dissipation caused by the viscous core. The correction process is iterative and affects the circulation at the blade elements and the evolution of trailed vortices.

The NWC is implemented in three versions of the PALM-FAST coupling: an ALM and two ASM variations, as listed in table 1. As the NWC was developed for an ALM, the first implementation in the PALM-FAST coupling is carried out for the model of an identical time step in FAST and PALM, i.e. an ALM.

The original code for the NWC corrects the wind speeds and calculates the corrected forces at the blades. In our case, the calculation of the forces is done by FAST and should remain there, since the extensive output of FAST is desired. Therefore, the NWC is implemented in such a way, that the wind speeds are being corrected and the corrected wind speeds are passed on to FAST. This means that the part of the NWC that corrects the wind speeds is called for each FAST time step on the PALM side. The calculation of the forces within the code of Meyer Forsting et al. (2020) is not used here. The corrected wind speeds are then sent from PALM to FAST as the current wind speed at the respective blade node positions.

https://doi.org/10.5194/wes-2024-146
Preprint. Discussion started: 2 December 2024

eawe european academy of wind energy
Open Access WIND ENERGY SCIENCE DISCUSSIONS

Table 1. Overview of the different models and their key differences.

	ALM (NWC)	ASM SWIRL	ASM-CL (NWC)	ASM-SL (NWC)
wind speed	wind speed in rotor area	wind speed in front of turbine + SWIRL	wind speed in rotor area	wind speed in rotor area
blade shape	lines	sector	sector	sector
method	BEM	per line in sector, transfer of wind speeds to FAST cf. Fig. 2a, correction by SWIRL FAST: BEM	per line in sector, transfer of wind speeds to FAST cf. Fig. 2a FAST: BEM	only wind speeds of first line is used cf. Fig. 2b FAST: BEM

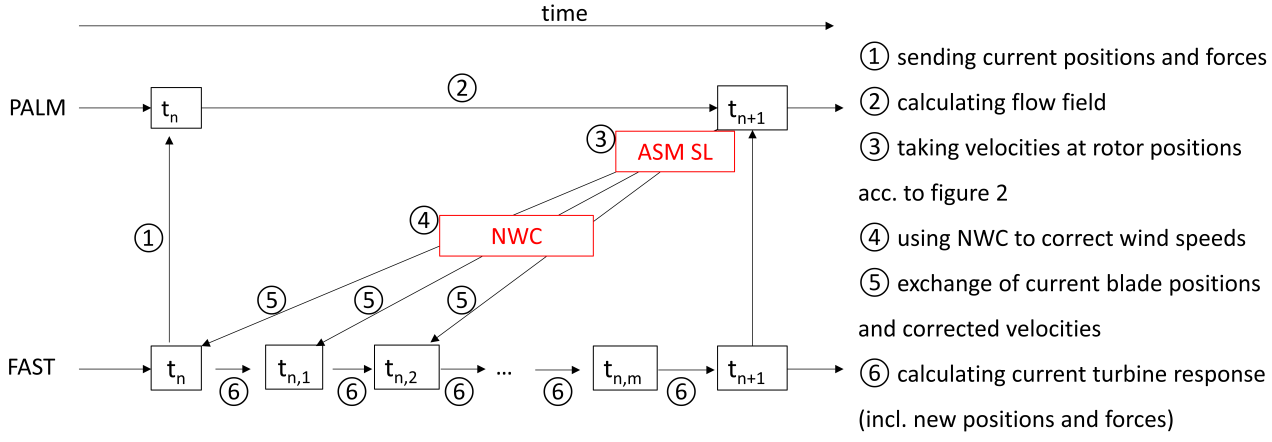

Figure 1. Schematic of the operation mode of the proposed coupling, the red fields show the points of change in comparison to ASM SWIRL.

Furthermore, the NWC is implemented in a sector method based on ASM SWIRL. A schematic of the working principle can be seen in Fig. 1. The ASM, instead of the ALM, on the PALM side is implemented to decouple the time stepping of FAST from PALM in order to make it computationally less expensive. While FAST is calculating usually with a time step smaller than an ALM model, i.e. ensuring that the chosen sampling rate covers the key frequencies of the system, the PALM time step is larger and set internally by PALM, determined either by the Courant–Friedrichs–Levy (CFL) criteria or the diffusion criteria, enabling the most efficient running of the LES code. PALM provides the wind speed information that FAST needs by using a frozen wind field. This means that PALM pauses its calculation until the FAST time matches the PALM simulation time.

https://doi.org/10.5194/wes-2024-146
Preprint. Discussion started: 2 December 2024

eawe european academy of wind energy
Open Access WIND ENERGY SCIENCE DISCUSSIONS

During this pause, the wind speeds from the previously calculated PALM time step are sent to FAST.

In ASM SWIRL the wind speed information is instead obtained from the free inflow in front of the turbine at the corresponding blade element positions in combination with using the FAST induction model SWIRL. Due to using wind speeds of the free inflow, the results obtained from this method include a temporal offset. This is because the wind speeds used for calculations reach the actual turbine at a later time.

Certain adjustments were necessary to successfully implement the NWC, the resulting variations are denoted as ASM-CL and ASM-SL. In the method proposed here, the wind speeds are taken in the rotor area and the induction model SWIRL is switched off. But the principle of the sector remains i.e. the wind field in PALM, which computes with a larger time step, is frozen, while FAST receives the wind speeds at the required positions from the frozen wind field until the simulation time of FAST reaches the ahead-running PALM time.

The distinction between ASM-CL and ASM-SL lies in the positions of where the wind speeds are extracted. The principle of ASM-CL is shown in Fig. 2a, where the new positions of the blades move away from the previously smeared forces in PALM until the current time in PALM is reached and a new wind field is computed. The previous sector, which is the area that the blade covers over one PALM time step, is indicated as light red. In this area and the surrounding grid points the forces have been smeared using a Gaussian shape. The influence of the introduced forces are highest close to this sector, meaning the blade position where the wind speed U_n is denoted. Therefore, the further the distance to the smearing of the previous time step, the less influence the previous forces have on the wind speeds, resulting in even higher wind speeds than in the ALM without NWC. Further corrections would be necessary to counteract the increased wind speeds due to the lack of influence of the forces, which is not pursued here.

The alternative approach, denoted as ASM-SL, is to use the wind speed positions where the previous force smearing has an influence (see Fig. 2b), meaning, that just the wind speeds are taken at the blade positions of the first FAST time step within a PALM time step, closest to the previously smeared forces and used for all the blade positions within the current sector. This was not necessary in the ASM SWIRL method, as the increasing distance to the previously projected forces was not a problem because the induction for the respective position was added using the SWIRL method.

For the simulations described here, revision 4901 of PALM and FAST v8 was used. A more detailed description of the used FAST settings can be seen in Krüger et al. (2022).

3 Investigation of the NWC method in ALM and ASM

3.1 Model verification in laminar flow

A laminar and homogeneous case with a constant wind speed of $8\,\mathrm{ms}^{-1}$ is considered, comparable to the simulations from (Meyer Forsting et al., 2019, 2020). In addition to the simulations with the described model framework, a standalone simulation of FAST, without coupling to PALM, is conducted and serves as a reference.

For the PALM simulation a resolution of $5\,\mathrm{m}$ and a grid size of 384×192 grid points in the horizontal direction and 192 with stretching of the grid in vertical direction is used and the boundary conditions are set to cyclic. More details of the set-up and

https://doi.org/10.5194/wes-2024-146
Preprint. Discussion started: 2 December 2024

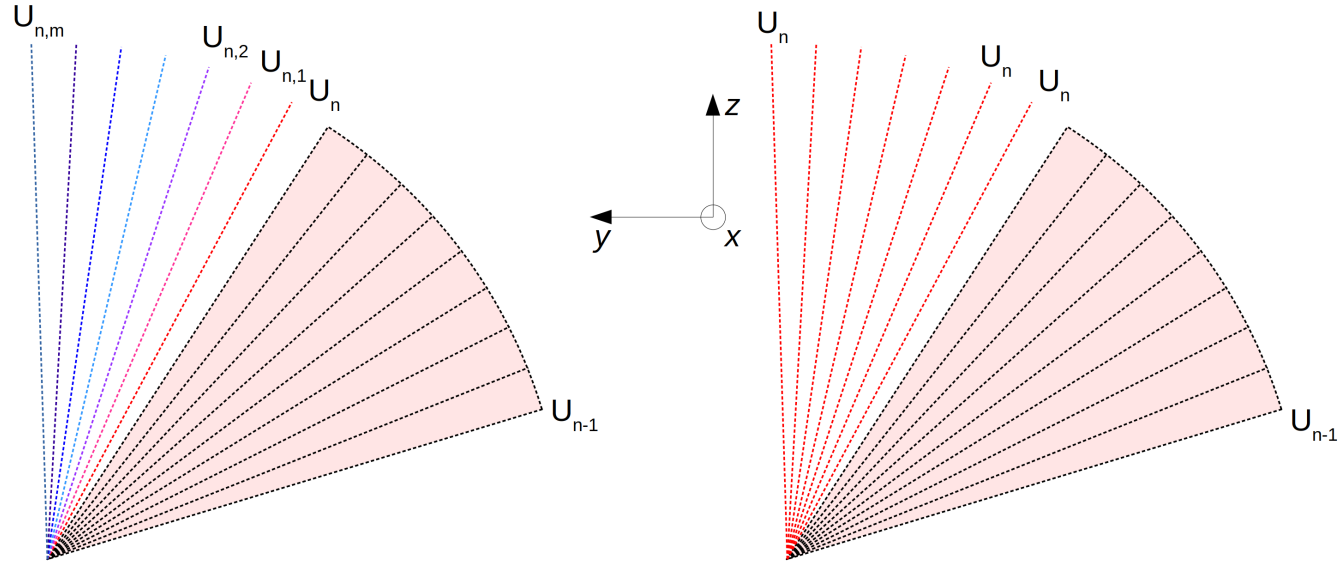

(a) ASM-CL (b) ASM-SL

Figure 2. Schematic of the two working principles of the described sector methods. (a) ASM-CL: Wind speeds U are taken at every blade position within the frozen wind field. The varying colours of $U_{n,m}$ represent different wind speeds, with reddish colours indicating a stronger influence from the previous time step and blue indicating a greater distance and therefore less influence from the previous time step. The previous PALM time step (= sector) is indicated in light red. (b) ASM-SL: Wind speeds U_n are taken at the first blade position with respect to the previous sector (light red) and used for all blade positions in the current sector.

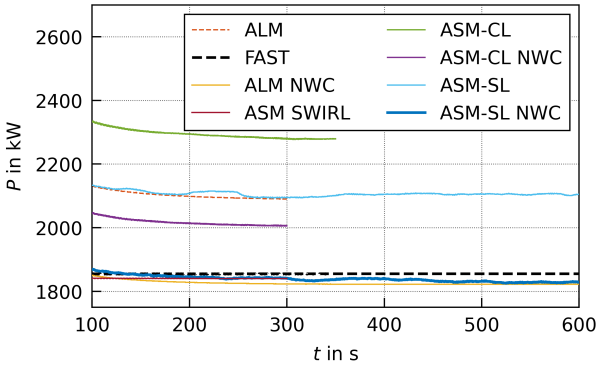

Figure 3. Comparison of ALM, ALM with NWC and ASM with NWC for the power output of the 5 MW NREL turbine in laminar conditions with 8 ms^{-1}.

the test case are provided in (Krüger et al., 2022).

The laminar case was simulated using different model variations: simulations of an ALM with and without NWC, the ASM-

https://doi.org/10.5194/wes-2024-146
Preprint. Discussion started: 2 December 2024

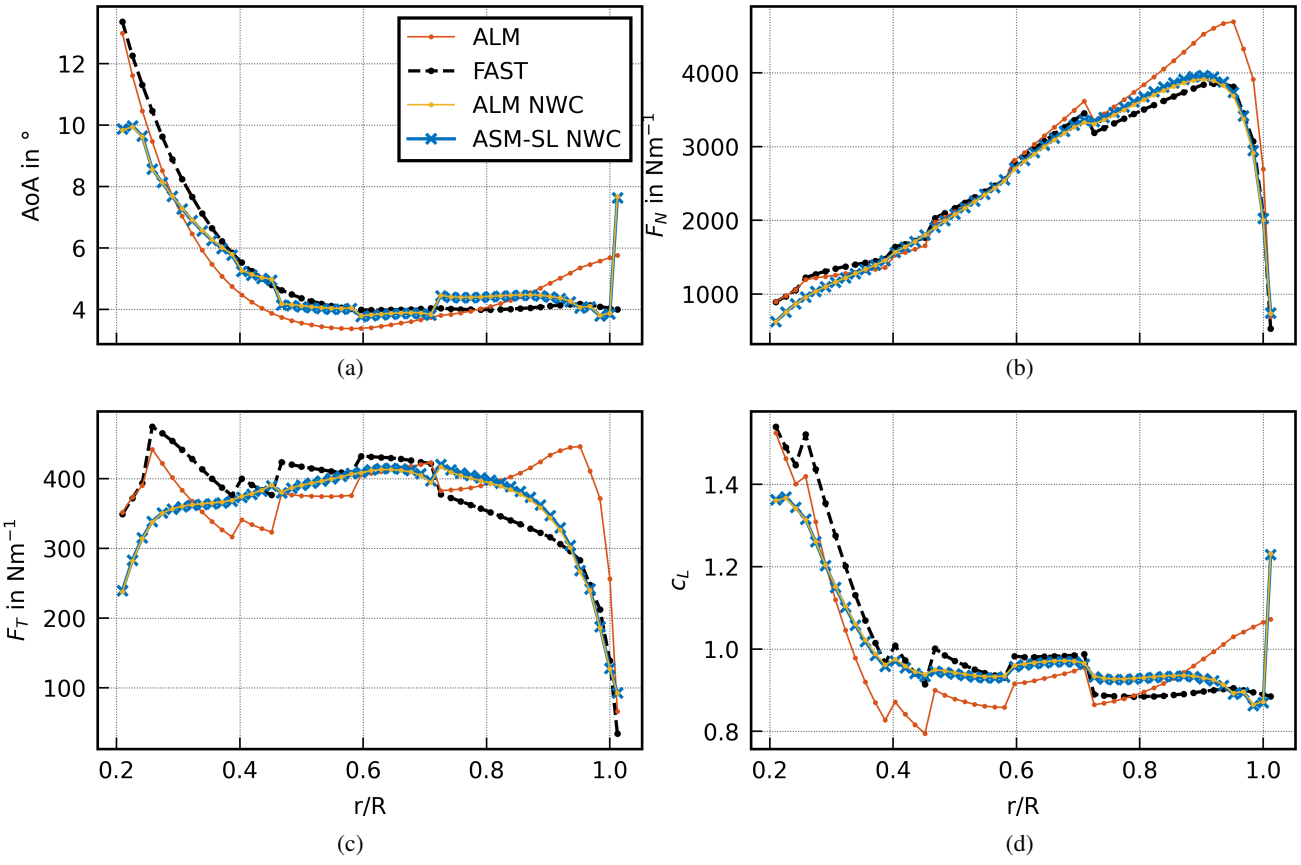

Figure 4. Comparison of (a) the angle of attack (b) the normal force along the blade normalized by the blade element width (c) the tangential force along the blade normalized by the blade element width and (d) the lift coefficient, averaged from 200 s until the end of the simulations, for an ALM without any correction, FAST, ALM with NWC and the ASM-SL with NWC.

CL with and without NWC and the ASM-SL with and without NWC were performed. In Fig. 3 the results of the power output after the initial turbine spin-up are shown. The first 100 s of the simulations show the spin-up of the turbine, which depends in all methods on the initialization values in FAST and is not considered of interest in this study. The simulation, denoted as FAST, which serves here as a reference, coincides with the published values for the NREL 5 MW turbine (Jonkman et al., 2009b). The ASM-CL (NWC) simulations were terminated early due to unpromising results, specifically a significant overestimation of power output, even with the NWC applied. Similarly, the ALM simulations were halted early for the same reason: an overestimation of power output. FAST yields a power output of 1855 kW after the turbine has fully adapted to the flow and its characteristics have reached a stationary state. The ALM without correction leads to a power value of 2090 kW, which is an overestimation of 13%. Using the NWC for the ALM lowers the power output.

The model ASM SWIRL (Krüger et al., 2022) reaches a good result compared to FAST. The power output of the ASM-CL

https://doi.org/10.5194/wes-2024-146
Preprint. Discussion started: 2 December 2024

eawe european academy of wind energy
Open Access WIND ENERGY SCIENCE DISCUSSIONS

is observed to be excessively high, primarily attributable to two factors. Firstly, the model partly lacks the influence of forces from the previous time step, thereby overestimating the wind speed, see e.g. Fig. 2a. Additionally, no correction for the missing induction is implemented. Using the NWC the power output can be lowered, yet it remains high due to the increasing distance from the forces exerted during the previous time step.

The power output of the ASM-SL coincides with the overestimated power output of the ALM. This is expected for the laminar case, as the distance between previous forces and new positions is the same in both models and both equally lack a further correction of the wind speeds. The ASM-SL (NWC) simulations seem to enhance small fluctuations of the power (see Fig. 3). This may be caused by the new method of extracting wind speeds from the frozen wind field (see Fig. 2b). It is possible that this method amplifies conditions, like structures in the wind field, that are already present in the wind speeds near the previous time step, as these wind speeds are used multiple times in FAST during one PALM time step. However, the variance remains small compared to the mean value. Simulations using the ASM-SL with NWC, denoted as ASM-SL NWC, agree well with the FAST reference curve and the mean power produced by the ALM NWC.

Displaying the parameters along the blade, as shown in Fig. 4a to Fig. 4d, motivated a deeper investigation into the relevance of the blade resolution, i.e. the number of blade elements. The findings can be found in Appendix A, showing a strong dependency of the results on the resolution specifically of the tip. Figures 4a to 4d shows the angle of attack, the forces and the lift coefficient across the blade, averaged from 200 s until the end of the simulations. Overall, the results of the ASM-SL NWC resemble the

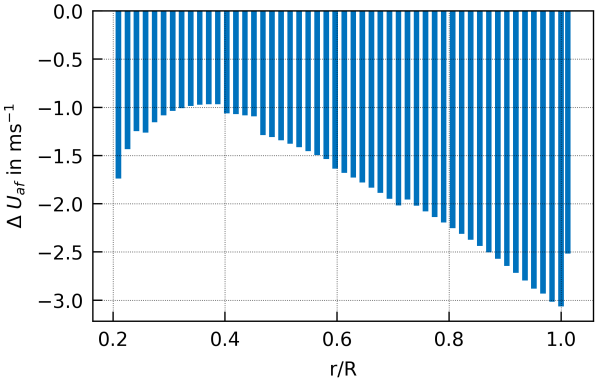

Figure 5. Wind speed difference between ASM-SL with and without NWC, averaged from 200 s until the end of the simulations.

ones of the ALM NWC with the corresponding 62 nodes very closely. Figures 4b and 4c show the normal and tangential forces acting along the blade in comparison for ALM, FAST, ALM NWC and ASM-SL NWC. The more smoothed curve of the forces of the corrected model variations in comparison to the ALM, correspond to the observations by Meyer Forsting et al. (2019) for the corrected ALM. For ALM and FAST, it is observed that the angle of attack has a smooth curve, while the forces and lift coefficient have a ragged curve. However, when the NWC is used, the forces show smoother curves and the angle of attack becomes ragged. This is likely related to the turbine model and the airfoil data, specifically the lift and drag coefficients. The NWC incorporates the same airfoil information, so that it is considered not only in FAST, but also in PALM in the calculations.

https://doi.org/10.5194/wes-2024-146
Preprint. Discussion started: 2 December 2024

eawe european academy of wind energy
Open Access WIND ENERGY SCIENCE DISCUSSIONS

This behavior could probably be improved by using a different interpolation method for the airfoil information, but it does not impact the quality of the presented results and is therefore not further investigated in this study. Additionally, Fig. 4d shows the lift coefficient, which is also influenced greatly by the NWC. In Appendix A similar plots for the dynamic pressure and the drag coefficients can be seen.

In Fig. 5 the effect of the NWC on the wind speeds along the blade is illustrated. The wind speed is reduced up to $3\,\mathrm{ms}^{-1}$ at the tip at a mean free stream velocity of $8\,\mathrm{ms}^{-1}$.

For the laminar inflow condition, we conclude, that the ASM-CL NWC resembles the results of the ALM NWC. Both models show results, that coincide well with the reference value of FAST on its own.

3.2 Model verification in turbulent flow

A key challenge for modelling an ASM in turbulent flows are the varying wind speeds within a computed sector. To evaluate the model's performance, a turbulent test case was simulated using LES, with an average wind speed of $7.4\,\mathrm{ms}^{-1}$ at hub height. With a resolution of $4\,\mathrm{m}$ and 1200×480 grid points in the horizontal directions and set to a neutral flow, meaning a constant potential temperature over height. For verification of the ASM-SL NWC, the ASM SWIRL model results serve as a reference and are plotted as a bold red line in Fig. 6.

Figure 6 shows that the obtained power time series of the ASM-SL concurs roughly with the course of the ALM. This is interesting in terms of the deficit that the ASM-SL might have due to using the same wind speeds multiple times within one sector, in contrast to the ALM, where new wind speeds are communicated for every FAST time step.

When using the NWC in case of the ASM-SL the power output is reduced and is similar to the power output of the ASM SWIRL, which has shown good results in comparison to measurement data. Therefore, it can be concluded that the ASM-SL NWC results in a reasonable power output even in a turbulent flow and is worth further testing and comparing to measurement data.

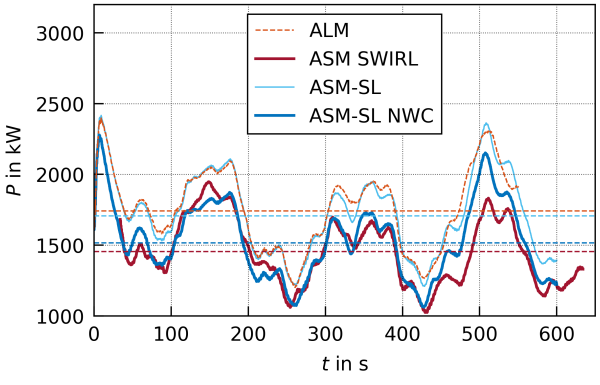

Figure 6. Comparison of different model variations for the power output of the 5 MW NREL turbine in turbulent conditions.

https://doi.org/10.5194/wes-2024-146
Preprint. Discussion started: 2 December 2024

eawe european academy of wind energy
Open Access WIND ENERGY SCIENCE DISCUSSIONS

3.3 Verification of the ASM-SL NWC in the wake of another turbine

In horizontally heterogeneous wind conditions the assumptions of the ASM SWIRL, using Taylor's frozen eddy hypothesis, are not valid anymore. As an example, a wake situation is simulated involving two eno114 3.5 MW turbines (denoted as: upstream T1, downstream T2) positioned in a straight line in the main wind direction. This situation is simulated both with the ASM SWIRL and with the ASM-SL NWC, whereby both turbines are simulated with the same model for each simulation. A turbine spacing of four rotor diameters is tested as well as eight rotor diameters, resulting in a total of four simulations. The flow in the LES was set to a neutral boundary layer, for more details see the case NBL in the section 4.

In this wake situation the model ASM SWIRL uses wind speeds from within the wake of T1, upstream of turbine T2, while the wake recovers until it reaches T2. This wake recovery is not taken into account in Taylor's frozen eddy hypothesis, leading to potentially too low wind speeds at the downstream turbine T2. As verification data, the PALM wind field at the position of T2 is extracted and used in combination with FAST, labeled as PALM wnd in Fig. 7a and Fig. 7b. For this, the wind fields at the position of T2 from simulations where only T1 is present are extracted and converted into a format suitable for input into a FAST simulation. This is a decoupled version of using PALM and FAST, there is no feedback from FAST to PALM and therefore no information about the downstream turbine in the wind field.

Figures 7a and 7b show the time series of the power output for the turbines T1 and T2 for the models ASM SWIRL, ASM-SL NWC and the reference PALM wnd. The time series for ASM SWIRL is time-shifted in the plot to make it comparable to the other methods. This adjustment accounts for wind speeds being taken in front of the turbine, causing the wind field structures to appear to reach the turbine earlier than in the actual wind field. It can be seen that the upstream turbine T1 (solid lines) react very similar to the inflow in both ASM models, which is consistent with the previously made observations (see section 3.2). The power output of the downstream turbine T2 (dashed lines) differs substantially, especially in the case of the narrow spacing. In the narrow turbine spacing, the wake recovery is less advanced before reaching the downstream turbines (Yang et al., 2015), highlighting the relevance to capture such effects in models.

It can also be observed that at T2, the differences between ASM SWIRL and the reference PALM wnd are greater than those between ASM-SL NWC and the reference. This result is plausible given the assumptions in ASM SWIRL and leads to the conclusion that the ASM-SL NWC model is better suited for delivering results in a wake situation. Figure 8 compares the power output statistics over a 600-second interval, starting at 100 s of simulation time. To ensure a fair comparison of the turbine reaction, for the calculation of the ASM SWIRL statistics the shifted time series is used, as it is also plotted in Fig. 7a and Fig. 7b. In addition to a difference in the means of the power output, there is also a difference in the standard deviation, which is an indicator of the turbulence intensity TI. The shape and magnitude of the ASM-SL NWC plot align well with the reference PALM wnd, indicating that a similar wind speed and TI were used to calculate the turbine power. However, the statistics of the ASM SWIRL differ from those of the PALM wnd. This discrepancy is due to not only the lower wind speed used in the calculation, which results in underestimated power, but also differences in other turbulence structures.

The reference PALM wind data, which represents the wind conditions and turbine response at position T2, closely matches

https://doi.org/10.5194/wes-2024-146
Preprint. Discussion started: 2 December 2024

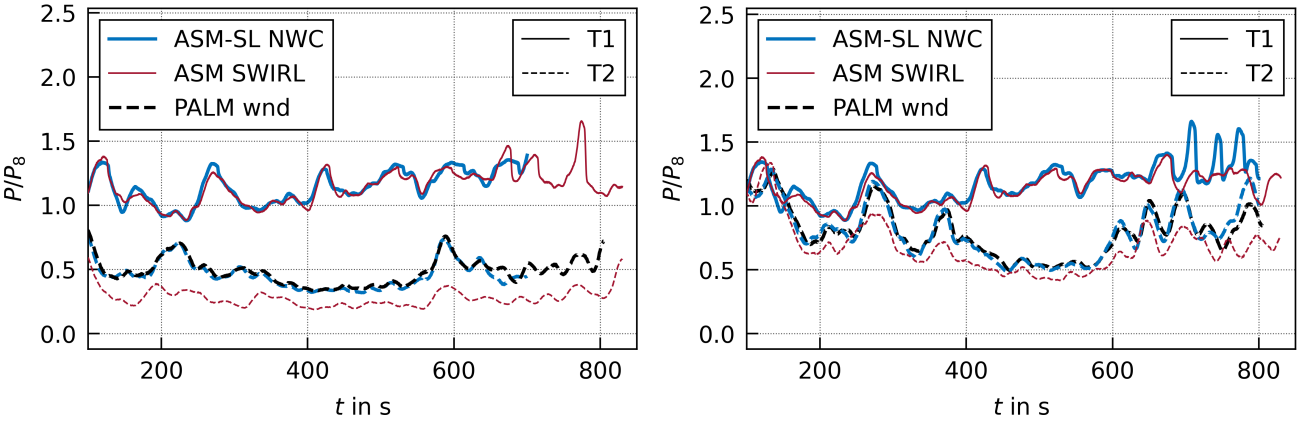

(a) $4D$ (b) $8D$

Figure 7. Comparison of power output for a wake situation with (a) a distance of $4D$ and (b) a distance of $8D$, the solid lines show the result of the upstream turbine T1, the dashed lines the downstream turbine T2. Additionally to the results of the sector models, results of a FAST simulation for T2 using an inflow field generated from the PALM wind field is shown in black.

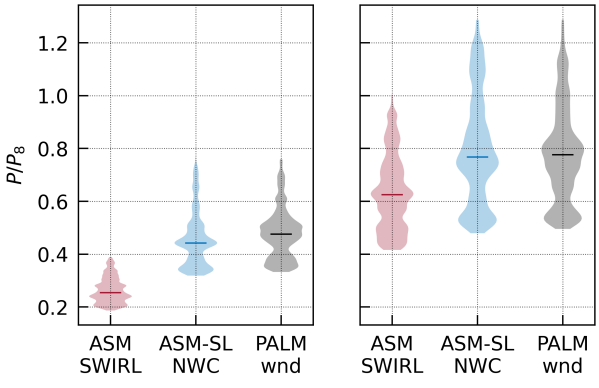

(a) $4D$ (b) $8D$

Figure 8. Comparison of the statistics of the normalized power time series of ASM SWIRL, ASM-SL NWC and PALM wnd for the turbine spacing of (a) $4D$ and (b) $8D$. Shown is the median and spread of the values of the above mentioned simulations.

the results of the ASM-SL NWC. Therefore, it can be concluded that the ASM-SL NWC is well-suited for modeling wake situations.

4 Validation with measurement data of a single eno114 3.5 MW turbine

This section compares the proposed modelling framework with measurements under free inflow conditions. This comparison with measurements is intended to determine whether the validation from Krüger et al. (2022) is transferable and also valid for

https://doi.org/10.5194/wes-2024-146
Preprint. Discussion started: 2 December 2024

eawe european academy of wind energy
Open Access WIND ENERGY SCIENCE DISCUSSIONS

the modelling framework presented here. In (Krüger et al., 2022), the presented coupling ASM SWIRL was compared to

Table 2. Setup of the precursor simulations: Size of the model domain in streamwise x, spanwise y and vertical z direction, grid size Δ, cooling rate $\Delta\Theta/\Delta t$, geostrophic wind speed components at the surface in x- and y-direction u_g, v_g and total simulated time t_{end}.

	x [m]	y [m]	z [m]	Δ [m]	$\Delta\Theta/\Delta t$ [K h^{-1}]	u_g [m s^{-1}]	v_g [m s^{-1}]	t_{end} [s]
NBL	5184	2304	2928	4	0	10.0	-4.25	93600
SBL	1440	960	616	4	-0.25	9.5	-5.17	46800

Table 3. Resulting flow parameters after reaching a stationary state in the precursor simulations, averaged over 3600 s: The magnitude of the wind speed at hub height averaged over the model domain U_{92m}, turbulence intensity calculated at one position in 92 m height TI_{92m}, shear parameter α (based on the power law $u_2 = u_1 \left(\frac{z_2}{z_1}\right)^{\alpha}$ for the relation of wind speeds at different heights), Obukhov length L in a height of 2.3 m (height is chosen for comparison to the eddy-covariance data at the measurement site) and boundary layer height z_i.

	U_{92m} [m s^{-1}]	TI_{92m} [%]	α [ ]	L [m]	z_i [m]
NBL	8.6	10.1	0.15	1228698	550
SBL	8.4	5.6	0.28	102	180

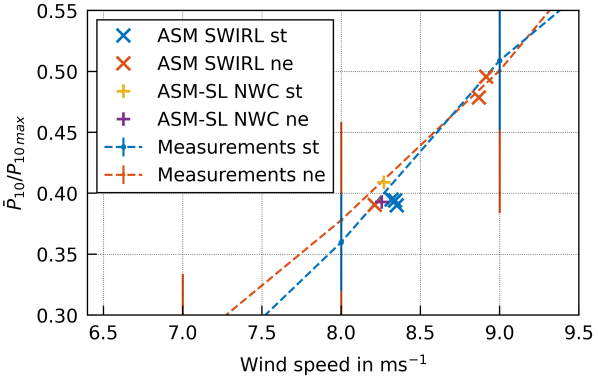

Figure 9. Extract of the power curve, normalised by the maximum 10 min power, determined from the measurement data, divided into stable (st) and neutral (ne) conditions. Comparison of the measurement data, the simulation data of ASM SWIRL and the new version ASM-SL NWC. The measurement and ASM SWIRL data are sourced from Krüger et al. (2022).

measurement data from an eno114 3.5 MW turbine located in northern Germany. The same simulation set-up is here used again to investigate how the ASM-SL NWC compares to the measurement data. For further information concerning the atmospheric conditions at the measurement site, how the simulations compare to them, and the comparability of the simulations with the

https://doi.org/10.5194/wes-2024-146
Preprint. Discussion started: 2 December 2024

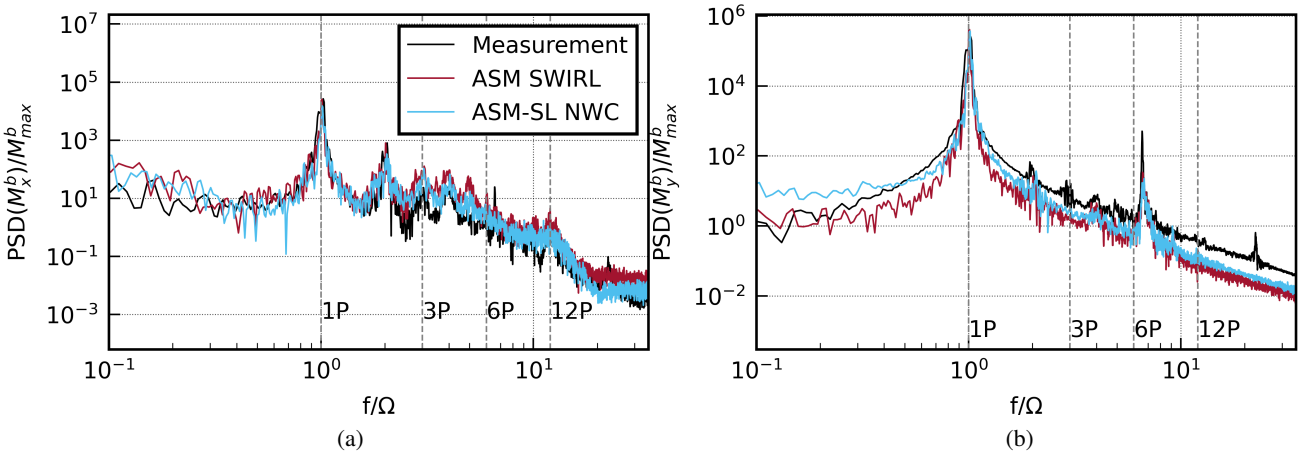

Figure 10. Spectrum of (a) the blade root bending moment out-of-plane M_y^b and (b) the blade root bending moment in-plane M_x^b. Comparison of measurement data and simulations of the models ASM SWIRL and ASM-SL NWC. The data are normalised by the maximum value of the blade root bending moment. The frequency is normalised by the rotor speed. The measurement and ASM SWIRL data are sourced from Krüger et al. (2022).

selected time interval of the measurement data, please refer to (Krüger et al., 2022). Idealized simulations were performed to match the prevailing inflow conditions of the eno114 3.5 MW turbine based on the measured data. One case with neutral and one case with stable stratification were simulated. The set-up of the precursor simulations is detailed in Table 2 and Table 3 shows the resulting atmospheric conditions. The precursor simulations are calculated with cyclic boundary conditions and no turbine in order to reach a stationary flow that can serve as a starting point for the simulations including a turbine.

In Fig. 9 the result of two simulations of the ASM-SL NWC can be seen in comparison to ASM SWIRL and the measurement data. No large deviations can be observed between the model versions. The stable case shows a slight increase in the power output of ASM-SL NWC compared to the simulations of the ASM SWIRL. This could be caused by the reduced mixing within a sector, which might have an effect due to the method of retrieving the wind speeds (c.f. Fig. 2a and b). However, the difference to the measurement data remains the same. Additionally, the performance of the new model version was analyzed using load data, with the blade loads illustrated in Fig. 10 as an example.

Overall, the ASM-SL NWC shows the same quality of performance as the ASM SWIRL for the selected case and a good agreement in comparison to the measurement data. For a more detailed analysis of the load spectra, please refer to Krüger et al. (2022). In summary, the existing differences in the spectra can be attributed to variations in the turbine model, such as a fixed blade imbalance and pitch offset between the blades in FAST, as well as discrepancies between the tower model and actual tower behaviour. Additionally, the 6P peak is significantly influenced by the shear over the rotor area, which varies slightly between the measurements and the simulations (see Appendix Krüger et al. (2022)). It can be concluded, that the validation of the simulation in Krüger et al. (2022) can be extended for the proposed method ASM-SL NWC.

https://doi.org/10.5194/wes-2024-146
Preprint. Discussion started: 2 December 2024

eawe european academy of wind energy
Open Access WIND ENERGY SCIENCE DISCUSSIONS

5 Conclusions

We developed a modelling framework capable of simulating atmospheric flows as well as providing detailed wind turbine dynamics and loads in a computationally efficient way. For this purpose, the ASM as presented in Krüger et al. (2022) was combined with the correction method NWC of Meyer Forsting et al. (2020).

To achieve the presented model framework, the NWC was implemented and examined in the ALM PALM-FAST coupling, which involves a coupled time step between FAST and PALM. Subsequently, to be able to use the NWC in the ASM, an extension to the sector model was developed and evaluated, denoted as ASM-SL (NWC). Comparisons of the models with each other and measured data of one eno114 3.5 MW turbine were performed. In addition, a wake situation with varying distances between turbines was investigated to test the effectiveness of the new coupling method.

The presented framework delivers good results in both laminar and turbulent test cases compared to their respective reference models. Wind speeds, which are otherwise too high and lead to overestimated power output, are accurately corrected by the NWC in the ASM-SL NWC. The good performance in the turbulent case verifies the spatial simplification, which the sector entails.

Furthermore, the ASM-SL NWC demonstrates superior performance in wake situations compared to the previously proposed coupling method. This makes the ASM-SL NWC a valuable tool for studying detailed turbine performance, including blade and tower loads, across a wide range of atmospheric flow conditions.

The comparisons of ASM-SL NWC to reference simulations yield favorable results, and validation with measurement data shows good agreement. This confirms the reliability of ASM-SL NWC in terms of both power output and load representation. The results strongly depend on the resolution of the blade, as found from the investigations of the NWC in the ALM coupling. Therefore, this is a crucial parameter for the quality of the simulation. While the resolution in the middle part of the blade and near the hub is less significant, a higher resolution at the blade tip yields better results.

In light of further developments, it is important to note that only situations within the mid-range wind speeds have been investigated thus far. Future testing should also include scenarios with lower and higher wind speeds, as these may involve different turbine control strategies.

On the technical side an upgrade from FAST v8 to OpenFAST and AeroDyn v15 is intended, as this promises further improvements of the aerodynamic calculations.

Code availability. The modified code for FAST v8, as well as the user code needed for the LES code PALM, will be made available once pending legal questions are clarified.

Data availability. The simulation and supervisory control and data acquisition (SCADA) data of the eno114 3.5MW turbine are confidential and therefore not available to the public.

https://doi.org/10.5194/wes-2024-146
Preprint. Discussion started: 2 December 2024

eawe european academy of wind energy
Open Access WIND ENERGY SCIENCE DISCUSSIONS

Appendix A: Investigation of the effect of the blade resolution of the NREL 5 MW turbine

When analysing the implementation of the NWC in the ALM, it was noticed that the course of the angle of attack along the blade in particular does not correspond to that in Meyer Forsting et al. (2019). The main difference in the set-ups of Meyer Forsting et al. (2019) and the ALM in this study is the resolution of the blade. For calculation of the forces and vortices along the blade, the turbine model needs to be set-up, dividing the blade into elements. Depending on the number of elements per blade, the resolution is higher or lower.

To study the impact of the blade resolution, we tested two additional resolutions. In addition to the 62 node blade used in the previous sections for the NREL 5 MW turbine, we investigated a coarser resolution of 17 nodes and one of 19 nodes. The case of 19 nodes is constructed, to test the importance of the resolution at particular the blade tip. As a basis, the blade with 17 nodes is utilized as the coarsest available set-up. To enhance the resolution at the blade tip, two additional elements are added, following the definition provided in the 62 blade nodes set-up. This results in a blade containing 19 blade nodes, however, this does not correspond to the used resolution of 19 nodes in Meyer Forsting et al. (2019), which was equally distributed along the blade.

The tested resolutions of 17, 19 and 62 nodes result in a power output of 1912 kW, 1846 kW and 1822 kW (see Table A1). These results lay close to the reference of the FAST simulation, i.e. an overestimation of 3.1% and an underestimation of 0.5% and 1.8% compared to the FAST reference simulation. The main differences lie at the tip, where the higher resolved blade, e.g. 62 nodes, captures more of the effects than the lower resolved blade, e.g. 17 nodes. The Fig. A1a to Fig. A1d show the angle of attack, forces and lift coefficient along the blade. The plots reflect the high impact of the NWC towards the blade tips, underlining also the importance the resolution at the blade tip.

The stand-alone FAST simulations were calculated with a resolution of 62 nodes per blade. The other resolutions of 17 and 19 nodes per blade were tested as well to determine the effect on the simulation which is regarded as the reference. The influence of the resolution can also be seen here, 17 nodes per blade yields a power of 1874 kW and 19 nodes per blade 1876 kW (see Fig. B1 in the Appendix). The difference between 17 and 19 nodes in comparison to 62 nodes per blade lie at about 1%. This should be kept in mind when regarding this as a reference, nevertheless the magnitude of the FAST stand-alone simulation can serve as a good indicator for the quality of the tested models. Since all simulations in Krüger et al. (2022) were carried out with a resolution of 62 blade nodes, the model with 62 nodes is also used in this study, in the ASM as well as in FAST, to ensure comparable simulations.

Appendix B: Power output of FAST depending on the blade resolution of the NREL 5 MW turbine

The following plots show the comparison of the FAST stand-alone simulations as well as the dynamic pressure and the drag coefficients along the blade in case of the laminar case described in section 3.

https://doi.org/10.5194/wes-2024-146
Preprint. Discussion started: 2 December 2024

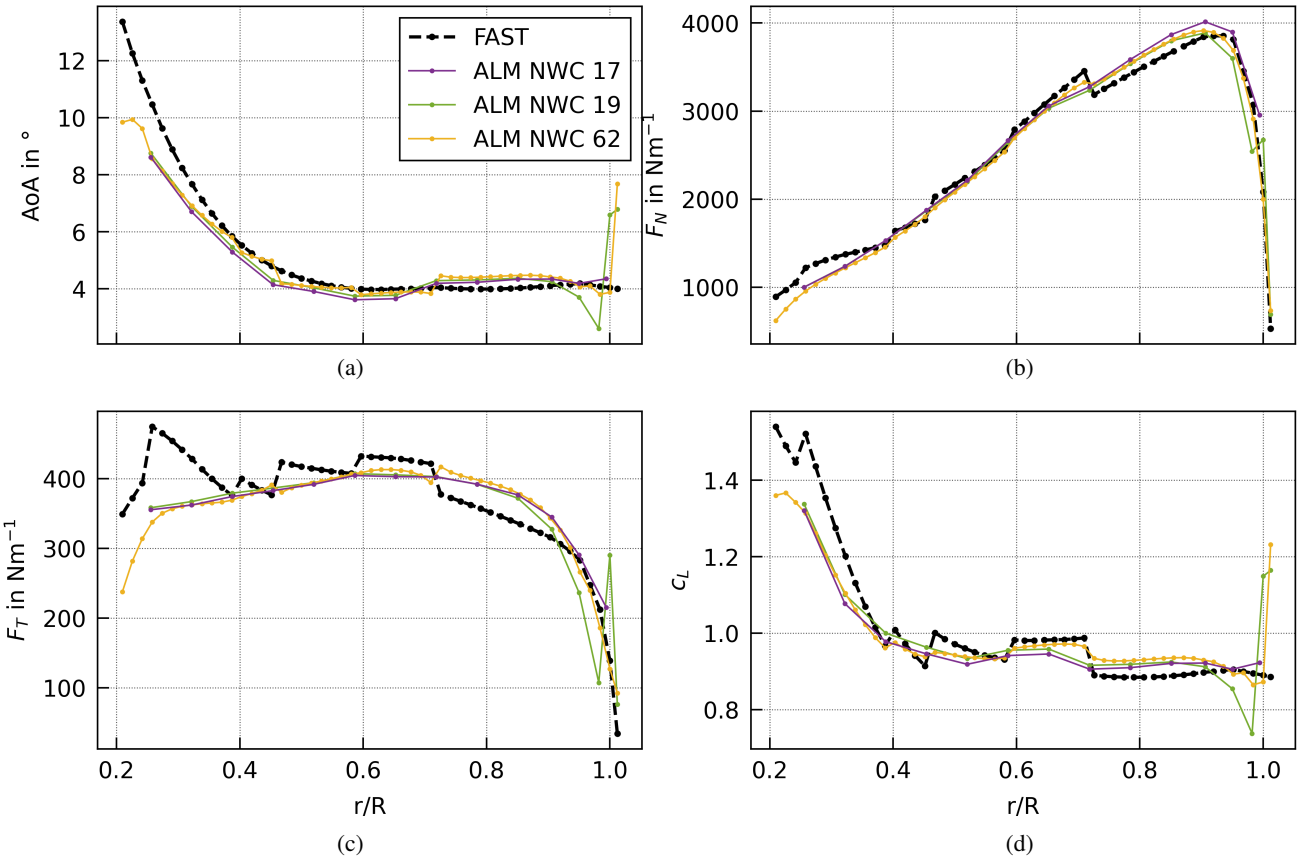

Figure A1. Comparison of (a) the angle of attack (b) the normal force along the blade normalized by the blade element width (c) the tangential force along the blade normalized by the blade element width and (d) the lift coefficient, averaged from 200 s until the end of the simulations, for FAST and the ALM NWC with the blade resolutions of 17, 19 and 62 nodes.

Author contributions. SoS developed the revised actuator sector method to make use of the NWC for the PALM–FAST coupling, performed the simulations and data analyses, and wrote the paper. TE implemented the NWC code into an ALM PALM-FAST coupling within the scope of a Master thesis, supervised by SoS. GS contributed to acquiring the funding for the work presented in the paper and provided intensive consultation on the development of the method and the scientific analyses. KA and LV provided intensive consultation on the scientific analyses and had a supervising function.

Competing interests. The authors declare that they have no conflict of interest.

https://doi.org/10.5194/wes-2024-146
Preprint. Discussion started: 2 December 2024

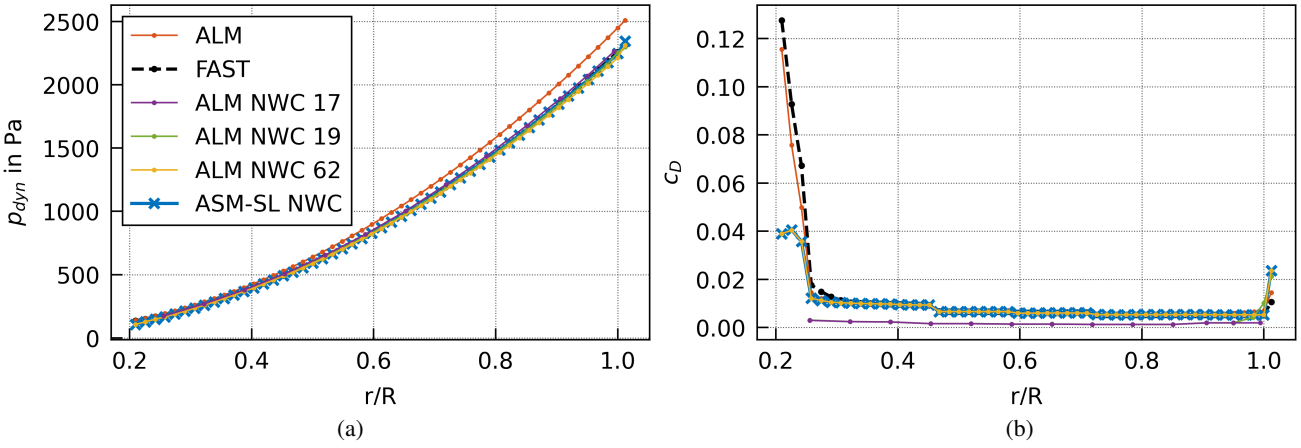

Figure A2. Comparison of (a) the dynamic pressure and (b) the drag coefficient, averaged from 200 s until the end of the simulations, for ALM, FAST and the ALM NWC with the blade resolutions of 17, 19 and 62 nodes, as well as ASM-SL NWC.

Table A1. Summary of the blade resolutions used in Meyer Forsting et al. (2019), denoted with M-F, and here, as well as their corresponding power output for a laminar case of 8 ms^{-1}.

Resolution	Description	Power at 8 ms^{-1} in kW
M-F 9	equally distributed along the blade	2130
M-F 19	equally distributed along the blade	1980
17	equally distributed along the blade	1912
19	17 nodes as basis, higher resolution at tip	1846
62	equally distributed along the blade	1822
FAST	using 62 equally distributed nodes	1855

Acknowledgements. The computations of the presented work were performed on the high-performance computing system EDDY of the University of Oldenburg funded by the Federal Ministry of Economic Affairs and Energy. The simulations were partly performed using the HPC Cluster MOUSE of the Carl von Ossietzky Universität Oldenburg (Germany) funded by the German Ministry of Economic Affairs and Climate Action (BMWK, grant no. 03EE3067A). We acknowledge the wind turbine manufacturer eno energy for providing SCADA data and the FAST turbine model, as well as for their support of the work.

https://doi.org/10.5194/wes-2024-146
Preprint. Discussion started: 2 December 2024

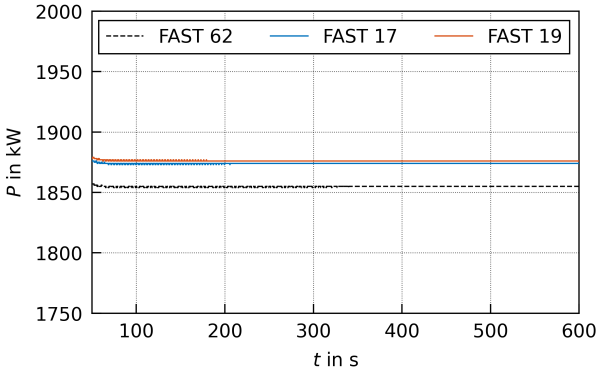

Figure B1. Power time series of the FAST stand-alone simulations with steady wind inflow conditions for the blade resolutions of 62, 17 and 19 nodes per blade.

References

Churchfield, M., Lee, S., Michalakes, J., and Moriarty, P. J.: A numerical study of the effects of atmospheric and wake turbulence on wind turbine dynamics, Journal of Turbulence, 13, 1–32, https://doi.org/https://doi.org/10.1080/14685248.2012.668191, 2012.

Dag, K.: Combined pseudo-spectral/actuator line model for wind turbine applications, Ph.D. thesis, DTU Wind Energy, 2017.

Doubrawa, P., Quon, E., Martínez-Tossas, L., Shaler, K., Debnath, M., Hamilton, N., Herges, T., Maniaci, D., Kelley, C., Hsieh, A., Blaylock, M., van der Laan, P., Andersen, S., Krueger, S., Cathelain, M., Schlez, W., Jonkman, J., Branlard, E., Steinfeld, G., Schmidt, S., Blondel, F., Lukassen, L., and Moriarty, P.: Multimodel validation of single wakes in neutral and stratified atmospheric conditions, Wind Energy, 23, 2027–2055, https://doi.org/https://doi.org/10.1002/we.2543, 2020.

Jonkman, J., Butterfield, S., Musial, W., and Scott, G.: Definition of a 5-MW Reference Wind Turbine for Offshore System Development, Tech. Rep. NREL/TP-500-38060, National Renewable Energy Laboratory, https://doi.org/https://doi.org/10.2172/947422, 2009b.

Jonkman, J. M. and Buhl Jr., M. L.: FAST User's Guide, Tech. Rep. NREL/EL-500-38230, National Renewable Energy Laboratory, 2005.

Krüger, S., Steinfeld, G., Kraft, M., and Lukassen, L.: Validation of a coupled atmospheric-aeroelastic model system for wind turbine power and load calculations, Wind Energ. Sci., 7, 323–344, https://doi.org/https://doi.org/10.5194/wes-7-323-2022, 2022.

Lamb, H.: Hydrodynamics, Cambridge University Press, 1932.

Maronga, B., Banzhaf, S., Burmeister, C., Esch, T., Forkel, R., Fröhlich, D., Fuka, V., Gehrke, K. F., Geletic, J., Giersch, S., Gronemeier, T., Groß, G., Heldens, W., Hellsten, A., Hoffmann, F., Inagaki, A., Kadasch, E., Kanani-Sühring, F., Ketelsen, K., Khan, B. A., Knigge, C., Knoop, H., Krc, P., Kurppa, M., Maamari, H., Matzarakis, A., Mauder, M., Pallasch, M., Pavlik, D., Pfafferott, J., Resler, J., Rissmann, S., Russo, E., Salim, M., Schrempf, M., Schwenkel, J., Seckmeyer, G., Schubert, S., Sühring, M., von Tils, R., Vollmer, L., Ward, S., Witha, B., Wurps, H., Zeidler, J., and Raasch, S.: Overview of the PALM model system 6.0, Geosci. Model Dev., 13, 1335–1372, https://doi.org/https://doi.org/10.5194/gmd-13-1335-2020, 2020.

Martínez-Tossas, L. A., Churchfield, M. J., and Meneveau, C.: Optimal smoothing length scale for Actuator line models of wind turbine blades based on Gaussian body force distribution, Wind Energ., 20, 1083–1096, 2017.

https://doi.org/10.5194/wes-2024-146
Preprint. Discussion started: 2 December 2024

Mehta, D., Van Zuijlen, A. H., Koren, B., Holierhoek, J., and Bijl, H.: Large Eddy Simulation of wind farm aerodynamics: A review, Journal of Wind Engineering and Industrial Aerodynamics, 133, 1–17, https://doi.org/https://doi.org/10.1016/j.jweia.2014.07.002, 2014.

Meyer Forsting, A., Pirrung, G., and Ramos-García, N.: A vortex-based tip/smearing correction for the actuator line, Wind Energ. Sci., 4, 369–383, https://doi.org/https://doi.org/10.5194/wes-4-369-2019, 2019.

Meyer Forsting, A., Pirrung, G., and Ramos-García, N.: Brief communication: A fast vortex-based smearing correction for the actuator line, Wind Energ. Sci., 5, 349–353, https://doi.org/https://doi.org/10.5194/wes-5-349-2020, 2020.

Mikkelsen, R.: Actuator Disc Methods Applied to Wind Turbines, Ph.D. thesis, Technical University of Denmark, 2003.

Mohammadi, M. M., Chanprasert, W., Olivares-Espinosa, H., and Ivanell, S.: An aeroelastic coupling of an actuator sector model with OpenFAST in atmospheric flows, Journal of Physics: Conference Series, 2767, 022 037, https://doi.org/10.1088/1742-6596/2767/2/022037, 2024.

Moriarty, P. J. and Hansen, A. C.: AeroDyn Theory Manual, Tech. Rep. NREL/TP-500-36881, National Renewable Energy Laboratory, https://doi.org/https://doi.org/10.2172/15014831, 2005.

Oseen, C. W.: Über Wirbelbewegung in einer reibenden Flüssigkeit, Arkiv för matematik, astronomi och fysik, 7, 14–21, https://doi.org/ISSN 0365-4133, 1911.

Pirrung, G., Madsen, H. A., Kim, T., and Heinz, J.: A coupled near and far wake model for wind turbine aerodynamics, Wind Energ., 19, 2053–2069, https://doi.org/https://doi.org/10.1002/we.1969, 2016.

Pirrung, G., Riziotis, V., Madsen, H. A., Hansen, M., and Kim, T.: Comparison of a coupled near- and far-wake model with a free-wake vortex code, Wind Energ. Sci., 2, 15–33, https://doi.org/https://doi.org/10.5194/wes-2-15-2017, 2017a.

Pirrung, G., Madsen, H. A., and Schreck, S.: Trailed vorticity modeling for aeroelastic wind turbine simulations in standstill, Wind Energ. Sci., 2, 521–532, https://doi.org/https://doi.org/10.5194/wes-2-521-2017, 2017b.

Storey, R., Cater, J., and Norris, S.: Large eddy simulation of turbine loading and performance in a wind farm, Renewable Energy, 95, 31–42, https://doi.org/https://doi.org/10.1016/j.renene.2016.03.067, 2016.

Storey, R. C., Norris, S. E., and Cater, J. E.: An actuator sector method for efficient transient wind turbine simulation, Wind Energy, 18, 699–711, https://doi.org/https://doi.org/10.1002/we.1722, 2015.

Sørensen, J. N. and Shen, W. Z.: Numerical modelling of wind turbine wakes, J. Fluid. Eng.-T. ASME, 124, 393–399, 2002.

Sørensen, J. N., Shen, W. Z., and Munduate, X.: Analysis of Wake States by a Full-feld Actuator Disc Model, Wind Energy, 1, 73–88, https://doi.org/https://doi.org/10.1002/(SICI)1099-1824(199812)1:2<73::AID-WE12>3.0.CO;2-L, 1998.

Taylor, G. I.: The spectrum of turbulence, Proceedings of the Royal Society A, 164, 476–490, 1938.

Troldborg, N.: Actuator Line Modelling of Wind Turbine Wakes, Ph.D. thesis, Technical University of Denmark, 2008.

Yang, X., Howard, K., Guala, M., and Sotiropoulos, F.: Effects of a three-dimensional hill on the wake characteristics of a model wind turbine, Physics of Fluids, 27, https://doi.org/https://doi.org/10.1063/1.4907685, 2015.